

Article

# New Cytotoxic Terpenoids from Soft Corals *Nephthea chabroli* and *Paralemnalia thyrsoides*

Yu-Sheng Lee <sup>1,†</sup>, Tsai-Hui Duh <sup>2,†</sup>, Shu-Sheng Siao <sup>1</sup>, Rey-Chang Chang <sup>3</sup>, Shang-Kwei Wang <sup>4,\*</sup> and Chang-Yih Duh <sup>1,\*</sup>

<sup>1</sup> Department of Marine Biotechnology and Resources, National Sun Yat-sen University, Kaohsiung 804, Taiwan; m995020028@student.nsysu.edu.tw (Y.-S.L.); m035020008@student.nsysu.edu.tw (S.-S.S.)

<sup>2</sup> Department of Medicinal and Applied Chemistry, Kaohsiung Medical University, Kaohsiung 807, Taiwan; tshudu@kmu.edu.tw

<sup>3</sup> Department of Marine Biotechnology, National Kaohsiung Marine University, Kaohsiung 811, Taiwan; rcchang@mail.nkmu.edu.tw

<sup>4</sup> Department of Microbiology, Kaohsiung Medical University, Kaohsiung 807, Taiwan

\* Correspondence: skwang@cc.kmu.edu.tw (S.-K.W.); yihduh@mail.nsysu.edu.tw (C.-Y.D.); Tel.: +886-7-312-1101 (ext. 2015) (S.-K.W.); +886-7-525-2000 (ext. 5036) (C.-Y.D.); Fax: +886-7-525-5020 (C.-Y.D.)

† These authors contributed equally to this work.

Received: 4 November 2017; Accepted: 11 December 2017; Published: 19 December 2017

**Abstract:** A novel cytotoxic diterpenoid, chabrolin A (**1**) (possessing an unprecedented terpenoid skeleton), as well as three new cytotoxic sesquiterpenoids, parathyrsoidins E–G (**2–4**), were isolated by cytotoxicity-guided fractionation from soft corals *Nephthea chabroli* and *Paralemnalia thyrsoides*. The structures of the new compounds were determined by extensive analysis of spectroscopic data.

**Keywords:** *Nephthea chabroli*; *Paralemnalia thyrsoides*; cytotoxicity

## 1. Introduction

Soft corals belonging to the genera *Nephthea* and *Paralemnalia* have proven to be a rich source of bioactive terpenoids [1–19]. In searching for bioactive compounds from marine organisms, the crude extracts of soft corals *Nephthea chabroli* and *Paralemnalia thyrsoides* have been found to exhibit cytotoxicity against murine lymphocytic leukemia cell line, with IC<sub>50</sub> values of 12.0 and 15.2 µg/mL, respectively. Cytotoxicity-guided fractionation of soft corals *N. chabroli* and *P. thyrsoides* led to the isolation and characterization of a novel cytotoxic diterpenoid, chabrolin A (**1**) (possessing an unprecedented terpenoid skeleton), as well as three new cytotoxic sesquiterpenoids, parathyrsoidins E–G (**2–4**) (Figure 1). The structures of these metabolites were established by extensive spectroscopic analysis.

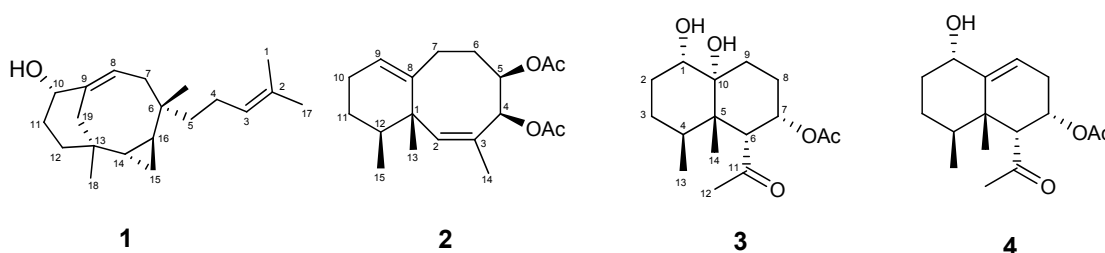
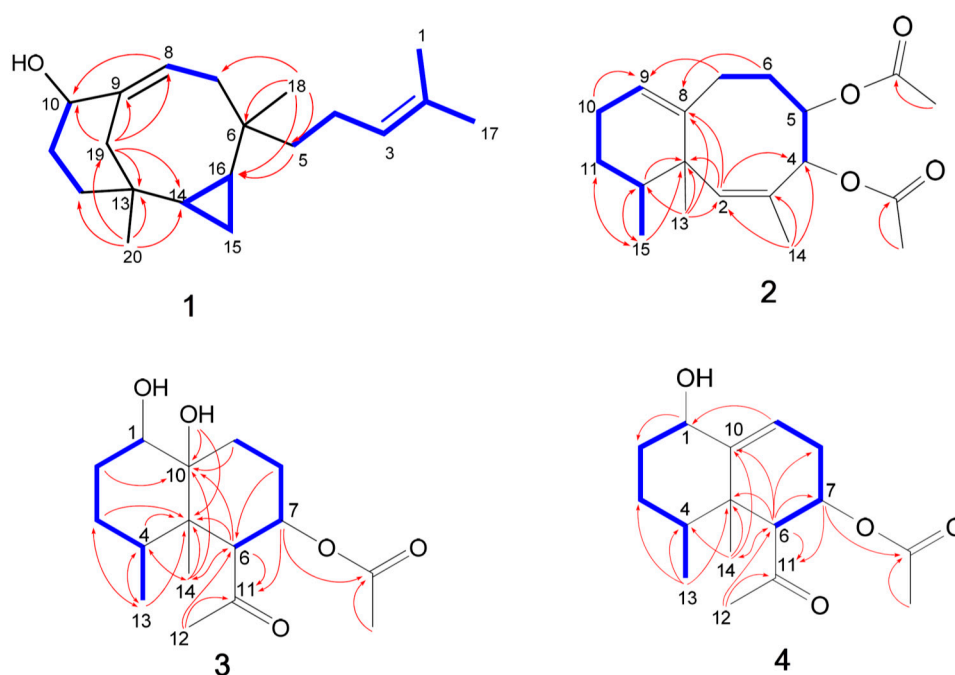


Figure 1. Structures of Metabolites 1–4.

## 2. Results and Discussion

The molecular formula of chabrolin A (**1**) was determined as  $C_{20}H_{32}O$  from its HR-FAB-MS,  $^{13}C$  NMR, and DEPT spectroscopic data. The  $^{13}C$  NMR (Figure S2) and DEPT spectrum of **1** exhibited the presence of four methyl, seven  $sp^3$  methylene, three  $sp^3$  methine, two  $sp^2$  methine, two  $sp^3$  quaternary, and two  $sp^2$  quaternary carbons. The presence of two trisubstituted olefins in **1** was shown by the NMR data [ $\delta_H$  5.59 t ( $J = 8.0$  Hz), 5.13 t ( $J = 7.2$  Hz);  $\delta_C$  144.5 C, 121.6 CH, 130.9 C, 125.3 CH] (Table 1). The NMR data [ $\delta_H$  0.25 dd ( $J = 15.2, 7.2$  Hz), 0.36 m, 0.49 m, 0.78 dd ( $J = 14.8, 7.2$  Hz);  $\delta_C$  8.6  $CH_2$ , 15.6 CH, 23.7 CH] (Table 1) pointed to a 1,2-disubstituted cyclopropane ring in **1**. The  $^1H$  NMR spectrum (Figure S1) displayed signals for four tertiary methyl groups, ( $\delta_H$  0.52, 0.64, 1.62, 1.69). The presence of the oxygen bearing  $sp^3$  methine ( $\delta_C$  74.1 CH) was shown in the  $^{13}C$  NMR spectrum. By interpretation of  $^1H$ - $^1H$  COSY correlations (Figure 2 and Figure S3), it was possible to establish four partial structures of contiguous proton systems extending from H-1 to H-5, from H-7 to H-8, from H-10 to H-12, and from H-14 to H-16. HMBC correlations (Figure S5) of (a)  $CH_3$ -18 to C-5, C-6, C-7, and C-16, (b)  $H_2$ -19 to C-8, C-9, C-10, C-13, and C-14, (c) H-8 to C-10, (d)  $CH_3$ -20 to C-12, C-13, C-14, and C-19 connected four partial structures concluding the planar structure of **1**, as shown in Figure 2. The above functionalities revealed that chabrolin A (**1**) possesses a novel diterpene tricyclic skeleton. The relative configuration of all chiral centers in **1** was deduced from a NOESY experiment (Figure S6). Assuming the  $\beta$ -orientation of  $H_3$ -18, NOESY correlations of  $H_3$ -18/H-15b,  $H_3$ -18/H-8, H-8/H-10, H-10/H-11b, H-11b/H-14, and H-14/H-15b suggested all to be on the  $\beta$  face of the molecule. NOESY correlations of H-15a/H-16, H-16/H-19a, H-15a/ $H_3$ -20, H-16/ $H_3$ -20, and  $H_2$ -19/ $H_3$ -20 suggested H-15a, H-16,  $H_2$ -19, and  $H_3$ -20 were on the  $\alpha$  face of the molecule (Figure 3).



**Figure 2.** Selected  $^1H$ - $^1H$  COSY (blue bold lines) and HMBC (red arrows) correlations of **1**–**4**.



**2** (Table 2 and Figure S8) displayed 19 carbon signals, and a DEPT experiments confirmed the presence of five methyl, four  $sp^3$  methylene, three  $sp^3$  methine, two  $sp^2$  methine, one  $sp^3$  quaternary, two  $sp^2$  quaternary, and two carbonyl carbons. The  $^{13}C$  and  $^1H$  NMR spectra (Figure S7) revealed the presence of two acetoxy groups [ $\delta_H$  2.03 (s),  $\delta_C$  20.8 (CH<sub>3</sub>), and 170.1 (CO);  $\delta_H$  2.06 (s),  $\delta_C$  21.2 (CH<sub>3</sub>), and 170.3 (CO)], two trisubstituted double bonds [ $\delta_H$  5.29 (brs),  $\delta_C$  137.9 (CH), and 128.0 (C);  $\delta_H$  5.57 (dd,  $J = 3.6, 3.2$  Hz),  $\delta_C$  125.9 (CH), and 141.0 (C)], and two oxygen-bearing methines [ $\delta_H$  5.18 (ddd,  $J = 9.2, 4.8, 3.2$  Hz),  $\delta_C$  74.7 (CH);  $\delta_H$  6.63 (d,  $J = 3.2$  Hz),  $\delta_C$  71.0 (CH)]. Thus, the bicyclic structure of **2** was revealed. From the  $^1H$ - $^1H$  COSY spectrum (Figure S9) of **2**, it was also possible to identify two different structural units (Figure 2), which were assembled with the assistance of HMBC experiments (Figure S11). Key HMBC correlations (Figure 2) from H-2 to C-1, C-4, C-8, C-13, and C-14, H<sub>2</sub>-6 to C-4, C-5, and C-8, H<sub>2</sub>-11 to C-1, C-9, C-10, and C-12, H<sub>3</sub>-13 to C-1, C-2, C-8, and C-12, H<sub>3</sub>-14 to C-2, C-3, and C-4, and H<sub>3</sub>-15 to C-1, C-11, and C-12 permitted the connection of the carbon skeleton. Thus, **2** was identified as a neolemnane-type new compound, on the basis of the above analysis and NMR data comparison with its stereoisomers, paralemnolins E and [9].

The *Z* geometry of the 2,3-double bond was established by a NOESY correlation (Figure S12) between H-2 and H<sub>3</sub>-14 and the relative configurations of all the chiral centers in **2** was established by analysis of NOESY correlations as shown in Figure 3. Assuming that the  $\beta$ -orientation of H<sub>3</sub>-13 ( $\delta$  1.05, s) and H<sub>3</sub>-13 showed NOESY correlations with H<sub>3</sub>-15 ( $\delta$  0.87, d,  $J = 6.8$  Hz), H-7 $\beta$  ( $\delta$  2.48, m), and H-2 ( $\delta$  5.29 brs), H<sub>3</sub>-15 and H-2 should also be positioned on the  $\beta$ -face. NOESY correlations observed from H-12 ( $\delta$  1.71 m) to H-4, H-6 $\alpha$  ( $\delta$  1.83, m) to H-5 ( $\delta$  5.18, ddd,  $J = 9.2, 4.8, 3.2$  Hz), and H-5 to H-4 ( $\delta$  6.63, d,  $J = 3.2$  Hz) reflected the  $\alpha$ -orientation of H-12, H-4, and H-5. Therefore, **2** was found to be the C-5 epimer of paralemnolin E [9].

Parathyrsoidin F (**3**) was obtained as a colorless oil. The HRESIMS of **3** established the molecular formula C<sub>16</sub>H<sub>26</sub>O<sub>5</sub>, implying four degrees of unsaturation. The DEPT spectrum (Table 2) of **3** evidenced four methyl, four  $sp^3$  methylene, three  $sp^3$  methine, two  $sp^3$  quaternary, and two carbonyl carbons. In turn, the  $^1H$  and  $^{13}C$  NMR (Tables 2 and 3) (Figures S13 and S14) spectra showed the presence of (a) a secondary methyl ( $\delta_C$  15.5 CH<sub>3</sub>;  $\delta_H$  0.35 d,  $J = 7.2$  Hz), (b) a tertiary methyl ( $\delta_C$  16.4 CH<sub>3</sub>;  $\delta_H$  0.54 s), (c) a secondary hydroxyl on C-1 ( $\delta_C$  71.7 CH;  $\delta_H$  3.32 brs), (d) a tertiary hydroxyl on C-10 ( $\delta_C$  72.6 C, 20.6 CH<sub>3</sub>;  $\delta_H$  1.52 s). IR absorption at 3421 cm<sup>-1</sup> and two absorptions at 1736 and 1714 cm<sup>-1</sup> and the NMR signals indicated the presence of a hydroxyl, an acetate, and a methyl ketone (Tables 2 and 3). The structure of **3** was determined by COSY (Figure 2 and Figure S15) and HMBC correlations (Figure 2 and Figure S17), and the latter correlations determined the acetate to be at C-7 (71.6 CH). The relative configuration of **3** was established from NOESY cross-peaks (Figure 3 and Figure S18). Assuming the  $\beta$ -orientation of H<sub>3</sub>-14 ( $\delta$  0.54 s), which exhibited NOESY correlations with H-1 ( $\delta$  3.32, d,  $J = 5.2$  Hz), H-6 ( $\delta$  2.99, d,  $J = 6.8$  Hz), H-7 ( $\delta$  5.16, ddd,  $J = 12.4, 6.8, 4.8$  Hz), and H<sub>3</sub>-13 ( $\delta$  0.35, d,  $J = 7.2$  Hz), the  $\beta$ -orientation of H-1, H-6, H-7, and H<sub>3</sub>-14 were suggested (Figure 3). One of the methylene protons at C-2 ( $\delta$  1.75, m) exhibited a NOESY correlation with H-1 and was identified as H-2 $\beta$ , while the other ( $\delta$  1.92, m) was assigned to H-2 $\alpha$ . The NOESY correlation observed between H-2 $\alpha$  and 10-OH ( $\delta$  6.68, d,  $J = 1.2$  Hz) indicated the  $\alpha$ -orientation of the 10-OH.

**Table 2.**  $^{13}\text{C}$  NMR spectral data of 2–4.

Position	2, $\delta_{\text{H}}^a$ (Type)	3, $\delta_{\text{H}}^b$ (Type)	4, $\delta_{\text{H}}^b$ (Type)
1	43.2, C	71.7, CH	68.9, CH
2	137.9, CH	30.86, CH <sub>2</sub>	35.8, CH <sub>2</sub>
3	128.0, C	29.0, CH <sub>2</sub>	28.7, CH <sub>2</sub>
4	71.0, CH	30.94, CH	35.4, CH
5	74.7, CH	46.1, C	43.9, C
6	30.2, CH <sub>2</sub>	59.5, CH	58.5, CH
7	31.2, CH <sub>2</sub>	71.6, CH	69.4, CH
8	141.0, C	23.1, CH <sub>2</sub>	27.4, CH <sub>2</sub>
9	125.9, CH	29.6, CH <sub>2</sub>	114.0, CH
10	23.1, CH <sub>2</sub>	72.6, C	143.6, C
11	26.2, CH <sub>2</sub>	214.3, C	206.9, C
12	38.3, CH	34.3, CH <sub>3</sub>	33.8, CH <sub>3</sub>
13	23.6, CH <sub>3</sub>	15.5, CH <sub>3</sub>	15.3, CH <sub>3</sub>
14	21.4, CH <sub>3</sub>	16.4, CH <sub>3</sub>	21.1, CH <sub>3</sub>
15	15.0, CH <sub>3</sub>	-	-
4-OAc	170.3, C 21.2, CH <sub>3</sub>	-	-
5-OAc	170.1, C 20.8, CH <sub>3</sub>	-	-
7-OAc	-	169.1, C 20.6, CH <sub>3</sub>	169.0, C 20.4, CH <sub>3</sub>

<sup>a</sup> Spectra were measured in CDCl<sub>3</sub> (100 MHz). <sup>b</sup> Spectra were measured in C<sub>6</sub>D<sub>6</sub> (100 MHz).

**Table 3.**  $^1\text{H}$  NMR spectral data of 2–4.

Position	2, $\delta_{\text{H}}^a$ (J in Hz)	3, $\delta_{\text{H}}^b$ (J in Hz)	4, $\delta_{\text{H}}^b$ (J in Hz)
1	-	3.52 d (5.2)	3.76 m
2	5.29 brs	$\alpha$ : 1.92 m; $\beta$ : 1.75 m	$\alpha$ : 1.13 m; $\beta$ : 1.73 m
3	-	$\alpha$ : 1.16 m; $\beta$ : 0.98 m	$\alpha$ : 1.13 m; $\beta$ : 1.04 m
4	6.63 d (3.2)	1.86 m,	1.63 m
5	5.18 ddd (9.2, 4.8, 3.2)	-	-
6	$\alpha$ : 1.83 m; $\beta$ : 1.94 m	2.99 d (6.8)	3.09 d (5.2)
7	$\alpha$ : 2.10 ddd (14.8, 12.4, 4.4); $\beta$ : 2.48 m	5.16 ddd (12.4, 6.8, 4.8)	5.38 ddd (10.0, 6.4, 5.2)
8	-	$\alpha$ : 1.92 m; $\beta$ : 1.64 ddt (12.4, 4.0, 4.0)	$\alpha$ : 2.42 m; $\beta$ : 2.34 m
9	5.57 dd (3.6, 3.2)	$\alpha$ : 2.22 ddd (14.0, 4.0, 4.0); $\beta$ : 1.42 td (14.0, 4.0)	5.67 dd (6.4, 2.8)
10	2.03 m	-	-
11	$\alpha$ : 1.78 m; $\beta$ : 1.39 m	-	-
12	1.71 m	1.82 s	1.96 s
13	1.05 s	0.35 d (7.2)	0.54 d (6.8)
14	1.68 d (1.2)	0.54 s	0.82 s
15	0.87 d (6.8)	-	-
4-OAc	2.06 s	-	-
5-OAc	2.03 s	-	-
7-OAc	-	1.52 s	1.63 s
12-OH	-	6.68 d (1.2)	-

<sup>a</sup> Spectra were measured in CDCl<sub>3</sub> (400 MHz). <sup>b</sup> Spectra were measured in C<sub>6</sub>D<sub>6</sub> (400 MHz).

The spectral evidence of parathyroidin G (4) (C<sub>16</sub>H<sub>24</sub>O<sub>4</sub>) suggested that this compound was a dehydrated form of 3.  $^1\text{H}$ - $^1\text{H}$  COSY correlations (Figure S21) from H-6 to H-9 through H-7 and H<sub>2</sub>-8 and from H-1 to H<sub>3</sub>-14 through H<sub>2</sub>-2, H<sub>2</sub>-3, and H-4, together with HMBC correlations from H<sub>3</sub>-13 to C-4, C-5, C-6, C-10, H-6 to C-5, C-7, C-8, C-10, and H-9 to C-1 (Figure 2 and Figure S23) and NOESY correlations (Figure 3 and Figure S24) between H<sub>3</sub>-13/H-1, H<sub>3</sub>-13/H-6, H<sub>3</sub>-13/H-7, H-6/H-7, and H-6/H<sub>3</sub>-14, confirmed that 4 was a dehydrated analogue of 3.

Cytotoxicity of Compounds 1–4 against the proliferation of a limited panel of cancer cell lines was evaluated against mouse lymphocytic leukemia (P-388), human colon adenocarcinoma (HT-29),

and human lung epithelial carcinoma (A-549). Compounds 1–4 displayed cytotoxicity against P-388, with ED<sub>50</sub> values of 3.18, 2.59, 3.31, and 2.49 µg/mL, respectively. However, Compounds 1–4 were not cytotoxic to A549 and HT-29 cell lines. Compounds 1–4 were also examined for the antiviral activity against human cytomegalovirus (HCMV), but none of them showed such activity.

### 3. Experimental Section

#### 3.1. General Experimental Procedures

Optical rotations were determined with a JASCO P1020 digital polarimeter (Tokyo, Japan). UV and IR spectra were obtained on JASCO V-650 (Tokyo, Japan) and JASCO FT/IR-4100 spectrophotometers (Tokyo, Japan), respectively. NMR spectra were recorded on a Varian MR 400 NMR spectrometer (Santa Clara, CA, USA) at 400 MHz for <sup>1</sup>H and 100 MHz for <sup>13</sup>C. <sup>1</sup>H NMR chemical shifts are expressed in δ (ppm) referring to the solvent peak δ<sub>H</sub> 7.27 for CHCl<sub>3</sub> or δ<sub>H</sub> 7.15 for C<sub>6</sub>D<sub>6</sub>, and coupling constants are expressed in Hertz (Hz). <sup>13</sup>C NMR chemical shifts are expressed in δ (ppm) referring to the solvent peak δ<sub>C</sub> 77.0 for CDCl<sub>3</sub> or δ<sub>C</sub> 128.0 for C<sub>6</sub>D<sub>6</sub>. MS were recorded by a Bruker APEX II mass spectrometer (Bruker, Bremen, Germany). Silica gel 60 (Merck, Darmstadt, Germany, 230–400 mesh) and LiChroprep RP-18 (Merck, 40–63 µm) were used for column chromatography. Precoated silica gel plates (Merck, Kieselgel 60 F<sub>254</sub>, 0.25 mm) and precoated RP-18 F<sub>254s</sub> plates (Merck) were used for thin-layer chromatography (TLC) analysis. High-performance liquid chromatography (HPLC) (Tokyo, Japan) was carried out using a Hitachi L-7100 pump (Tokyo, Japan) equipped with a Hitachi L-7400 UV detector (Tokyo, Japan) at 220 nm together with a semi-preparative reversed-phased column (Merck, Hibar LiChrospher RP-18e, 5 µm, 250 mm × 25 mm).

#### 3.2. Animal Material

The octocoral *N. chabroli* was collected by hand using scuba at Green Islang, Taitong County, Taiwan, in August 2015, at a depth of 6 m. A voucher specimen (GN-100) was deposited in the Department of Marine Biotechnology and Resources, National Sun Yat-sen University.

The octocoral *P. thyrsoides* was collected by hand using scuba at San-Hsian-Tai, Taitong County, Taiwan, in July 2008, at a depth of 6 m. A voucher specimen (SST-07) was deposited in the Department of Marine Biotechnology and Resources, National Sun Yat-sen University.

#### 3.3. Extraction and Separation

The frozen soft coral was chopped into small pieces and extracted with acetone in a percolator at room temperature. The acetone extract of *N. chabroli* was concentrated to a brown gum, which was partitioned with EtOAc and H<sub>2</sub>O. The EtOAc-soluble residue (50 g) was subjected to Si 60 CC using *n*-hexane–EtOAc mixtures of increasing polarity for elution. Fraction 10, eluted with *n*-hexane–EtOAc (1:10), was purified by reverse-phase HPLC (MeOH–H<sub>2</sub>O, 85:15) to afford 1 (2.9 mg).

The frozen soft coral was chopped into small pieces and extracted with acetone in a percolator at room temperature. The acetone extract of *P. thyrsoides* was concentrated to a brown gum, which was partitioned with EtOAc and H<sub>2</sub>O. The EtOAc-soluble residue (10 g) was subjected to Si 60 CC using *n*-hexane–EtOAc mixtures of increasing polarity for elution. Fraction 8, eluted with *n*-hexane–EtOAc (30:1), was purified by reverse-phase HPLC (MeOH–H<sub>2</sub>O, 95:5) to afford 2 (3.0 mg). Fraction 15, eluted with *n*-hexane–EtOAc (1:1), was purified by reverse-phase HPLC (MeOH–H<sub>2</sub>O, 55:45) to afford 3 (3.0 mg) and 4 (1.0 mg).

**Chabrolin A (1):** Colorless amorphous solid;  $[\alpha]_D^{25} = +102$  (c 0.1, CHCl<sub>3</sub>); IR (neat) ν<sub>max</sub> 3439, 2965, 1635, and 772 cm<sup>-1</sup>; <sup>1</sup>H NMR data, see Table 1; <sup>13</sup>C NMR data, see Table 2; ESIMS *m/z* 311 [M + Na]<sup>+</sup>; (+)-HRESIMS *m/z* 311.23465 (calcd. for C<sub>20</sub>H<sub>32</sub>ONa, 311.23454).

**Parathyroidin E (2):** Colorless amorphous solid;  $[\alpha]_D^{25} = -25$  (c 0.3, CHCl<sub>3</sub>); IR (neat) ν<sub>max</sub> 2964, 2927, 1743, 1455, 1369, 1247, and 871 cm<sup>-1</sup>; <sup>1</sup>H NMR data, see Table 1; <sup>13</sup>C NMR data, see Table 2; ESIMS *m/z* 343 [M + Na]<sup>+</sup>; (+)-HRESIMS *m/z* 343.1887 (calcd. for C<sub>19</sub>H<sub>28</sub>O<sub>4</sub>Na, 343.1885).

*Parathyrsoidin F (3)*: Colorless amorphous solid;  $[\alpha]_D^{25} = -54$  (*c* 0.3, CHCl<sub>3</sub>); IR (neat)  $\nu_{\max}$  3421, 2926, 1736, 1714, 1376, 1245, 1111, and 859 cm<sup>-1</sup>; <sup>1</sup>H NMR data, see Table 1; <sup>13</sup>C NMR data, see Table 2; ESIMS *m/z* 321 [M + Na]<sup>+</sup>; (+)-HRESIMS *m/z* 321.1676 (calcd. for C<sub>16</sub>H<sub>26</sub>O<sub>5</sub>Na, 321.1678).

*Parathyrsoidin G (4)*: Colorless amorphous solid;  $[\alpha]_D^{25} = -87$  (*c* 0.1, CHCl<sub>3</sub>); IR (neat)  $\nu_{\max}$  3421, 2964, 1739, 1714, 1362, 1236, and 869 cm<sup>-1</sup>; <sup>1</sup>H NMR data, see Table 1; <sup>13</sup>C NMR data, see Table 2; ESIMS *m/z* 303 [M + Na]<sup>+</sup>; (+)-HRESIMS *m/z* 303.1573 (calcd for C<sub>16</sub>H<sub>24</sub>O<sub>4</sub>Na, 303.1572).

### 3.4. Cytotoxicity Assay

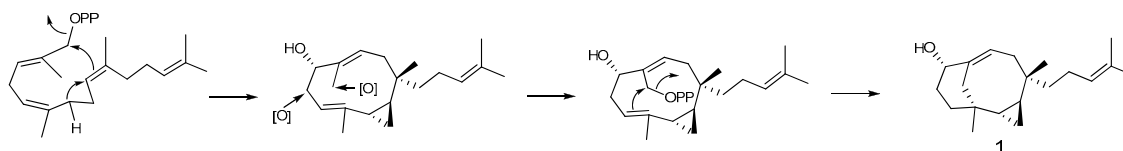
Cytotoxicity was determined on P-388 (mouse lymphocytic leukemia), HT-29 (human colon adenocarcinoma), and A-549 (human lung epithelial carcinoma) tumor cells using a modification of the MTT colorimetric method according to a previously described procedure [20,21]. The provision of the P-388 cell line was supported by J.M. Pezzuto, formerly of the Department of Medicinal Chemistry and Pharmacognosy, University of Illinois at Chicago. HT-29 and A-549 cell lines were purchased from the American Type Culture Collection. To measure the cytotoxic activities of tested compounds, five concentrations with three replications were performed on each cell line. Mithramycin was used as a positive control.

### 3.5. Anti-HCMV Assay

To determine the effects of natural products upon the HCMV cytopathic effect (CPE), confluent human embryonic lung (HEL) cells grown in 24-well plates were incubated for 1 h in the presence or absence of various concentrations of tested natural products with three replications. Ganciclovir was used as a positive control. Then, cells were infected with HCMV at an input of 1000 pfu (plaque forming units) per well of a 24-well dish. Antiviral activity was expressed as IC<sub>50</sub> (50% inhibitory concentration), or a compound concentration required to reduce virus-induced CPE by 50% after 7 days as compared with the untreated control. To monitor the cell growth upon treating with natural products, an MTT-colorimetric assay was employed [22].

## 4. Conclusions

Cytotoxicity-guided fractionation of the ethyl acetate extract of the soft corals *N. chabroli* and *P. thyrsoides* led to the isolation of a novel diterpenoid, chabrolin A (**1**) (possessing an unprecedented terpenoid skeleton) as well as three new sesquiterpenoids. Compounds **1–4** displayed cytotoxicity against P-388, with ED<sub>50</sub> values of 3.18, 2.59, 3.31, and 2.49 µg/mL, respectively. However, Compounds **1–4** were not cytotoxic to A549 and HT-29 cell lines and did not show anti-HCMV activity. A plausible biosynthetic pathway of **1** is proposed in Scheme 1.



**Scheme 1.** A plausible biosynthetic pathway of **1**.

**Supplementary Materials:** NMR spectra of new compounds **1–4** are available online at [www.mdpi.com/1660-3397/15/12/392/s1](http://www.mdpi.com/1660-3397/15/12/392/s1), Figure S1. <sup>1</sup>H NMR spectrum (400 MHz) of chabrolin A (**1**) in CDCl<sub>3</sub>; Figure S2. <sup>13</sup>C NMR spectrum (100 MHz) of chabrolin A (**1**) in CDCl<sub>3</sub>; Figure S3. COSY spectrum (400 MHz) of chabrolin A (**1**) in CDCl<sub>3</sub>; Figure S4. HSQC spectrum (400 MHz) of chabrolin A (**1**) in CDCl<sub>3</sub>; Figure S5. HMBC spectrum (400 MHz) of chabrolin A (**1**) in CDCl<sub>3</sub>; Figure S6. NOESY spectrum (400 MHz) of chabrolin A (**1**) in CDCl<sub>3</sub>; Figure S7. <sup>1</sup>H NMR spectrum (400 MHz) of parathyrsoidin E (**2**) in CDCl<sub>3</sub>; Figure S8. <sup>13</sup>C NMR spectrum (100 MHz) of parathyrsoidin E (**2**) in CDCl<sub>3</sub>; Figure S9. COSY spectrum (400 MHz) of parathyrsoidin E (**2**) in CDCl<sub>3</sub>; Figure S10. HSQC spectrum (400 MHz) of parathyrsoidin E (**2**) in CDCl<sub>3</sub>; Figure S11. HMBC spectrum (400 MHz) of parathyrsoidin E (**2**) in CDCl<sub>3</sub>; Figure S12. NOESY spectrum (400 MHz) of parathyrsoidin E (**2**) in CDCl<sub>3</sub>; Figure S13. <sup>1</sup>H NMR spectrum (400 MHz) of parathyrsoidin F (**3**) in C<sub>6</sub>D<sub>6</sub>; Figure S14. <sup>13</sup>C NMR spectrum

(100 MHz) of parathyroidin F (3) in C6D6; Figure S15. COSY spectrum (400 MHz) of parathyroidin F (3) in C6D6; Figure S16. HSQC spectrum (400 MHz) of parathyroidin F (3) in C6D6; Figure S17. HMBC spectrum (400 MHz) of parathyroidin F (3) in C6D6; Figure S18. NOESY spectrum (400 MHz) of parathyroidin F (3) in C6D6; Figure S19. <sup>1</sup>H NMR spectrum (400 MHz) of parathyroidin G (4) in C6D6; Figure S20. <sup>13</sup>C NMR spectrum (100 MHz) of parathyroidin G (4) in C6D6; Figure S21. COSY spectrum (400 MHz) of parathyroidin G (4) in C6D6; Figure S22. HSQC spectrum (400 MHz) of parathyroidin G (4) in C6D6; Figure S23. HMBC spectrum (400 MHz) of parathyroidin G (4) in C6D6; Figure S24. NOESY spectrum (400 MHz) of parathyroidin G (4) in C6D6.

**Acknowledgments:** This research was financially supported by grants from Ministry of Science and Technology. (MOST105-2320-B-110-003-MY3), NSYSUNKMU Joint Project (106-P010), and NSYSUKMU Joint Project (106-P016). We thank Chang-Feng Dai, Institute of Oceanography, National Taiwan University, for the identification the soft corals.

**Author Contributions:** Chang-Yih Duh, Shang-Kwei Wang and Rey-Chang Chang conceived and designed the experiments; Yu-Sheng Lee, Tsai-Hui Duh and Shu-Sheng Siao performed the experiments.

**Conflicts of Interest:** The authors declare no conflict of interest.

## References

1. Duh, C.-Y.; Wang, S.-K.; Weng, Y.-L.; Chiang, M.Y.; Dai, C.-F. Cytotoxic terpenoids from the Formosan Soft Coral *Nephthea brassica*. *J. Nat. Prod.* **1999**, *62*, 1518–1521. [[CrossRef](#)] [[PubMed](#)]
2. Duh, C.-Y.; Wang, S.-K.; Weng, Y.-L. Brassicolene, a novel cytotoxic diterpenoid from the Formosan soft coral *Nephthea brassica*. *Tetrahedron Lett.* **2000**, *41*, 1401–1404. [[CrossRef](#)]
3. Kitagawa, I.; Cui, Z.; Son, B.W.; Kobayashi, M.; Kyogoku, Y. Marine natural products. 17. Nephtheoxydiol, a new cytotoxic hydroperoxy-germacrane sesquiterpene, and related sesquiterpenoids from an Okinawan soft coral of *Nephthea* sp. (*Nephtheidae*). *Chem. Pharm. Bull.* **1987**, *35*, 124–135. [[CrossRef](#)] [[PubMed](#)]
4. El-Gamal, A.A.H.; Wang, S.-K.; Dai, C.-F.; Chen, I.-C.; Duh, C.-Y. Prenylbicyclgermacrane diterpenoids from the Formosan soft coral *Nephthea pacifica*. *J. Nat. Prod.* **2005**, *68*, 74–77. [[CrossRef](#)] [[PubMed](#)]
5. El-Gamal, A.A.H.; Wang, S.-K.; Duh, C.-Y. Prenylbicyclgermacrane diterpenoids from the Formosan Soft coral *Nephthea elongatae*. *Chem. Pharm. Bull.* **2007**, *55*, 890–893. [[CrossRef](#)] [[PubMed](#)]
6. Su, J.-Y.; Zhong, Y.-L.; Zeng, L.-M. Two new sesquiterpenoids from the soft coral *Paralemmalia thyrsoides*. *J. Nat. Prod.* **1993**, *56*, 288–291. [[CrossRef](#)]
7. Bowden, B.F.; Coll, J.C.; Mitchell, S.J. Studies of Australian soft corals. XIX. Two new sesquiterpenes with the nardosinane skeleton from a *Paralemmalia* species. *Aust. J. Chem.* **1980**, *33*, 885–890. [[CrossRef](#)]
8. Izac, R.R.; Schneider, P.; Swain, M.; Fenical, W. New nor-sesquiterpenoids of apparent nardosinane origin from the pacific soft-coral *Paralemmalia thyrsoides*. *Tetrahedron Lett.* **1982**, *23*, 817–820. [[CrossRef](#)]
9. Huang, H.-C.; Chao, C.-H.; Su, J.-H.; Hsu, C.-H.; Chen, S.-P.; Kuo, Y.-H.; Sheu, J.-H. Neolemnane-type sesquiterpenoids from a Formosan soft coral *Paralemmalia thyrsoides*. *Chem. Pharm. Bull.* **2007**, *55*, 876–880. [[CrossRef](#)] [[PubMed](#)]
10. Huang, C.-Y.; Su, J.-H.; Chen, B.-W.; Wen, Z.-H.; Dai, C.-F.; Shen, J.-H.; Sung, P.-J. Nardosinane-type sesquiterpenoids from the Formosan soft coral *Paralemmalia thyrsoides*. *Mar. Drugs* **2011**, *9*, 1543–1553. [[CrossRef](#)] [[PubMed](#)]
11. Cheng, S.-Y.; Lin, E.-H.; Huang, J.-S.; Wen, Z.-H.; Duh, C.-Y. Ylangene-type and nardosinane-type sesquiterpenoids from the soft corals *Lemnalia flava* and *Paralemmalia thyrsoides*. *Chem. Pharm. Bull.* **2010**, *58*, 381–385. [[CrossRef](#)] [[PubMed](#)]
12. Bishara, A.; Yeffet, D.; Sisso, M.; Shmul, G.; Schleyer, M.; Benayahu, Y.; Rudi, A.; Kashman, Y. Nardosinanol A–I and lemnafricanol, sesquiterpenes from several soft corals, *Lemnalia* sp., *Paralemmalia clavata*, *Lemnalia Africana*, and *Rhytisma fulvum fulvum*. *J. Nat. Prod.* **2008**, *71*, 375–380. [[CrossRef](#)] [[PubMed](#)]
13. Zeng, L.-M.; Zhong, Y.-L.; Su, J.-Y.; Zhao, D. Sesquiterpenes from the soft coral *Paralemmalia thyrsoides* and their biogenetic correlation. *Chin. Sci. Bull.* **1995**, *40*, 213–216.
14. Wang, G.-H.; Huang, H.-C.; Su, J.-H.; Wu, Y.-C.; Sheu, J.-H. Paralemmolins J–P, new sesquiterpenoids from the soft coral *Paralemmalia thyrsoides*. *Chem. Pharm. Bull.* **2010**, *58*, 30–33. [[CrossRef](#)] [[PubMed](#)]
15. Huang, H.-C.; Chao, C.-H.; Liao, J.-H.; Chiang, M.Y.; Dai, C.-F.; Wu, Y.-C.; Sheu, J.-H. A novel chlorinated norsesquiterpenoid and two related new metabolites from the soft coral *Paralemmalia thyrsoides*. *Tetrahedron Lett.* **2005**, *46*, 7711–7714. [[CrossRef](#)]

16. Huang, H.-C.; Wen, Z.-H.; Chao, C.-H.; Ahmed, A.F.; Chiang, M.Y.; Kuo, Y.-H.; Hsu, C.-H.; Chen, S.-P.; Sheu, J.-H. Novel sesquiterpenoids from the Formosan soft coral *Paralemnalia thyrsooides*. *Tetrahedron Lett.* **2006**, *47*, 8751–8755. [[CrossRef](#)]
17. Dalozé, D.; Braekman, J.C.; Georget, P.; Tursch, B. Chemical studies of marine invertebrates. XXII. Two novel sesquiterpenes from soft corals of the genera *Lemnalia* and *Paralemnalia*. *Bull. Soc. Chim. Belg.* **1977**, *86*, 47–54. [[CrossRef](#)]
18. Wang, S.-K.; Lee, Y.-S.; Duh, C.-Y. Paralemnolide A, an unprecedented bisnorsesquiterpene from the Taiwanese soft coral *Paralemnalia thyrsooides*. *Mar. Drugs* **2012**, *10*, 1528–1535. [[CrossRef](#)] [[PubMed](#)]
19. Tseng, Y.-J.; Lee, Y.-S.; Wang, S.-K.; Duh, C.-Y. Parathyrsoidins A–D, Four new sesquiterpenoids from the soft coral *Paralemnalia thyrsooides*. *Mar. Drugs* **2013**, *11*, 2501–2509. [[CrossRef](#)] [[PubMed](#)]
20. Hou, R.-S.; Duh, C.-Y.; Chiang, M.Y.; Lin, C.-N. Sinugibberol, a new cytotoxic cembranoid diterpene from the soft coral *Sinularia gibberosa*. *J. Nat. Prod.* **1995**, *58*, 1126–1130. [[CrossRef](#)] [[PubMed](#)]
21. Geran, R.I.; Greenberg, N.H.; MacDonald, M.M.; Schumacher, A.M.; Abbott, B.J. Protocols for screening chemical agents and natural products against animal tumors and other biological systems. *Cancer Chemother. Rep.* **1972**, *3*, 1–103.
22. Stevens, M.; Balzarini, J.; Tabarrini, O.; Andrei, G.; Snoeck, R.; Cecchetti, V.; Fravolini, A.; de Clercq, E.; Pannecouque, C. Cell-dependent interference of a series of new 6-aminoquinolone derivatives with viral (HIV/CMV) transactivation. *J. Antimicrob. Chemother.* **2005**, *56*, 847–855. [[CrossRef](#)] [[PubMed](#)]



© 2017 by the authors. Licensee MDPI, Basel, Switzerland. This article is an open access article distributed under the terms and conditions of the Creative Commons Attribution (CC BY) license (<http://creativecommons.org/licenses/by/4.0/>).